Defining the degree of fracturing in fault zones: implications in the study of landslide susceptibility

Davide Vianello[1]

[1] Department of Earth Science, University of Torino, Torino 10125, Italy.

ID DV, 0000-0002-2075-6687.

SOCIETÀ GEOLOGICA ITALIANA
FONDATA NEL 1881 - ENTE MORALE R. D. 17 OTTOBRE 1885

ABSTRACT

This contribute describes the fracture network of rock masses along a section normal to two parallel faults between Claviere and Cesana Torinese (Western Alps), applying traditional scanline method, topological analysis and geomechanical classification by Geological Strength Index. Based on the variation of fracture intensity defined by topology, the aim of this study is to estimate the width of the zones with a more pervasive fracturing around the faults. These zones could be considered as a reference to define the average "buffer zone" of the analysed fault system in landslide susceptibility studies at regional scale. In the studied area, the fracture intensity is derived from topological analysis (i.e., total length of fractures per unit area – P21 values) abruptly increases in areas 200 to 400 metres-wide adjacent to the considered faults with values of fracture intensity greater than 20 m/m2 and 70 m/m2 respectively. The geomechanical GSI classification underlies a coherent variation in the degree of fracturing in the analysed areas close to the faults.

KEY-WORDS: fracture network, fault zone, topological analysis, GSI index, scanline method.

INTRODUCTION

In studies of landslide susceptibility such as those related to debris flow, geological, morphological, and hydrological parameters are the main predisposing factors to be considered (e.g., Varnes, 1978; Van Westen, 1993). Predisposing geological parameters include basement, quaternary deposits and structures reported on geological maps, among others. The degree of fracturing of the rock mass plays an important role in the production of loose material potentially involved in debris flows and should therefore always be considered in landslide susceptibility studies.

In defining susceptibility maps at a regional scale, the occurrence of highly fractured rock masses is mainly considered within "buffer zones" (i.e., zones of more pervasive fracturing with respect to adjacent ones) along faults reported in available geologic maps (e.g., Saha et al., 2005; He et al., 2008; Ilia et al., 2016; Nohani et al., 2019; Wen et al., 2022 and reference herein). However, sizes of these buffer zones are often arbitrary, often poorly constrained by field data and usually considered homogeneous for the different systems of faults traced in the geological maps.

Different approaches have been proposed in the literature to define the degree of fracturing at regional scale and to provide a fracturing map. The application of remote sensing techniques, widely used in landslide susceptibility assessment to produce thematic layers (i.e., cover vegetations, landslide source area, debris deposits) could provide in large areas information on potential lineaments network (Jordan et al., 2005; Bonetto et al., 2015, 2017, 2021; Umili et al., 2013, 2018). However, for a more accurate interpretation of fracturing degree of rock masses, analysis at the outcrop scale is certainly the optimal methodology.

At the outcrop scale, many different methods exist for fracture data collection. Generally, four main sampling strategies are applied: the linear scanline method (Priest & Hudson, 1981; Priest, 1993), areal sampling (Wu & Pollard, 1995), rectangular window sampling (Pahl, 1981; Priest, 1993) and the circular scanline method (Mauldon et al., 2001; Rohrbaugh et al., 2002).

In the frame of an ongoing research aimed to develop and test a method for susceptibility mapping considering semi-quantitative interaction of several predisposing parameters (Bonetto et al., 2021; Vianello et al., 2022), the present contribution investigates the fracturing degree of rock masses across mapped faults in

the Upper Susa Valley (Western Alps). The aim of the present study is to recognize variation of degree of fracturing in order to define the width of buffer zones (i.e., zone of increasing pervasive fracturing) around the considered faults, and apply them to realize susceptibility map. Here, features of the fracture network (inclusive of all the mechanical discontinuities of the rock mass) were defined by linear scanline method and topological analysis (i.e., Sanderson & Nixon, 2015). To this purpose, fracture intensity (i.e., total length of fractures per unit area; see Sanderson & Nixon, 2015) and the rock mass structure described by Geological Strength Index (GSI - i.e., Hoek, 1994; Hoek et al., 1998; Marinos & Hoek, 2000) are considered important attributes of fracture network to be defined.

GEOLOGICAL SETTING

The Alpine belt is the product of the collision of the European and Adriatic tectonic plates. The plate convergence was responsible for the closure of the interposed Tethyan ocean, opened in Mesozoic times, and was followed by continental collision. Hence, the Alpine belt consists of tectonically juxtaposed continental and oceanic derived units (Dal Piaz, 2010).

The area investigated in this study is located between Claviere and Cesana Torinese (upper Susa Valley, Fig 1) and is part of the axial sector of the Western Alps. In the northern sector of the studied area, the continental pre-Piemonte Chaberton-Grand Hoche unit tectonically juxtaposed above the Lago Nero and other units belonging to the oceanic Piemonte-Liguria zone, while in the southern sector the same Lago Nero unit is overlaid by the Chenaillet unit (Servizio Geologico D'Italia, 2020) (Fig. 1). The Chaberton unit consists of a thick succession of Triassic dolomitic marble and Lower-Middle Jurassic calcschist with phyllite and levels of metabreccias of dolostone and basement rocks. The Lago Nero unit consists of serpentinite and meta-basalt wrapped by meta-ophicalcites, overlain by radiolarian meta-chert (Upper Jurassic), marble, and by a succession of prevailing calcschist with levels of marble and black metapelite (Cretaceous). The Chenaillet unit consists of pillow lavas overlying gabbroic rocks and serpentinized mantle.

At a map scale, a major strike-slip high-angle fault zone with NE-SW trend (and identified by two linked main faults on Fig. 1) divides a northern sector with Lago Nero unit overlaid by Chaberton unit from a southern sector with Lago Nero unit under the Chenaillet unit.

METHODS FOR FRACTURE SAMPLING

Fracture data were collected on accessible outcrops defining a 2000 m-long section normal to the fault traces (Fig. 1). Fractures were classified according to their dominant mode of wall rock movement and filling, i.e., joints (or extension fractures, with no or undetectable shear displacement), faults or shear fractures (shearing modes), and veins (generally opening mode fractures with filling) (i.e., Peacock et al., 2018). At each sampling site, the
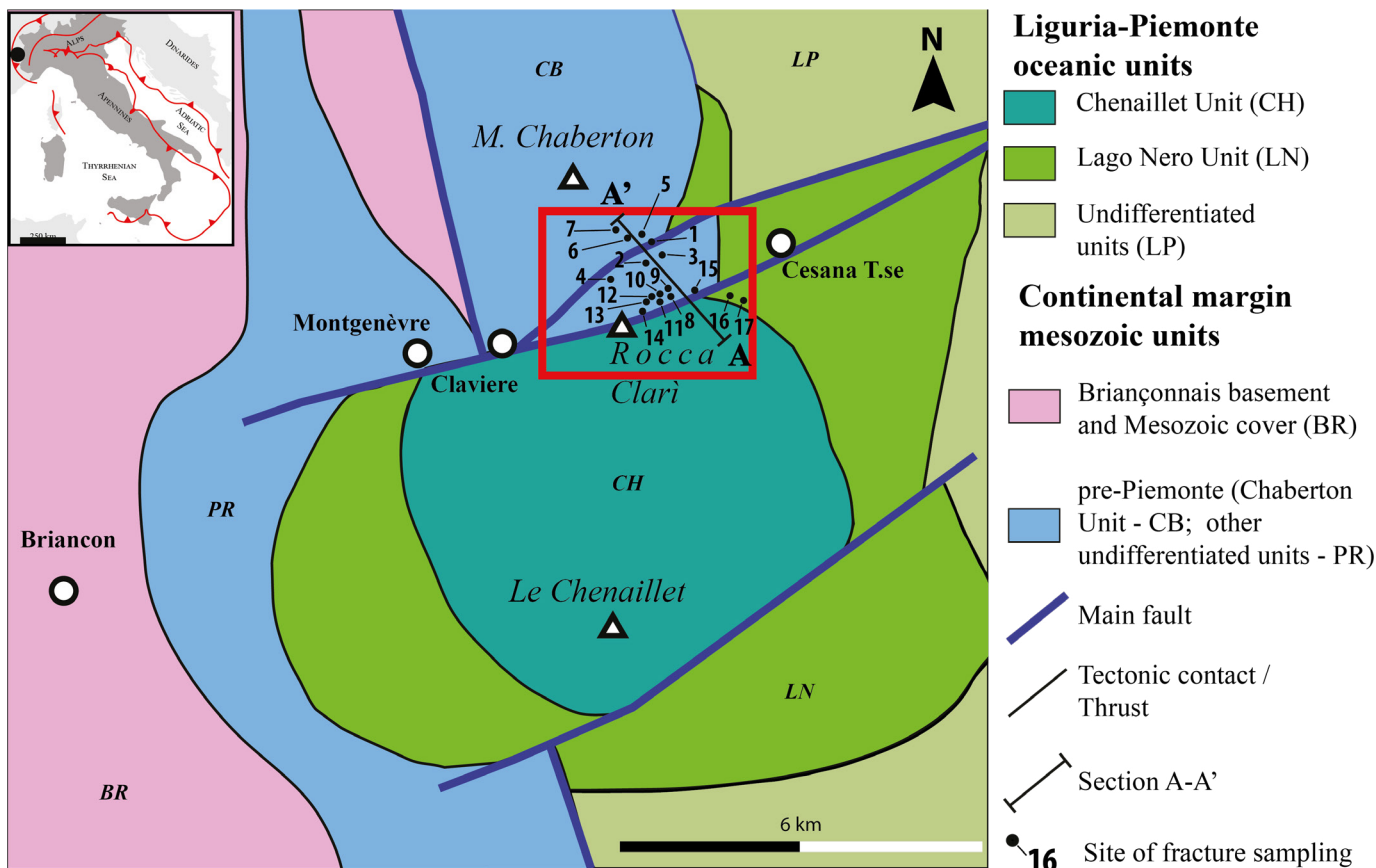

Fig. 1 - Simplified tectonic map of the sector of the Western Alps where is located the investigated area (red rectangle). Simplified after Servizio Geologico D'Italia, 2020.

scanline method was applied to define fracture attributes based on the International Society for Rock Mechanics - ISRM (1978) advice. This method is easy and rapid for recording a wide range of fracture attributes and requires laying a tape on an outcrop and collecting all intersecting fractures. Each sampled fracture has been then classified as joint, fault or vein and described by orientation (dip direction, dip), aperture and eventual filling (i.e., clay filling). This step of the study allowed to obtain a robust statistical dataset of different type of fractures and their attributes.

The arrangement and geometric relationships of the fractures were defined by topological analysis as proposed by Sanderson and Nixon (2015). The topological analysis of the fracture network treats the fractures as lines formed by one (for isolated fractures) or more branches (if fracture is intersecting or abuts with other fractures), which have a node at each end. The node is classified as I-node for isolated tips, X-node for crossing fractures and Y-node for abutments. Because the branches are composed by nodes consequently, branches can be classified into three topological groups: I-I (isolated) branches, I-C (partly connected) branches, and C-C (doubly fully connected) branches. The proportion of node and branch plotted on a triangular diagram provides the basis for describing the topology of a fracture network. Starting from topological analyses, the 2D-fracture intensity (total trace length per unit area, P_{21}) for each considered site is given by $P_{21}=N_L L_C/Area$ (with N_L the number of fractures and L_C the characteristic length, most simply defined as the arithmetic mean of the line lengths) or, considering branches, $B_{21}=N_B B_C/Area$ (with N_B is the number of such branches and B_C is the average branch length), with $P_{21}=B_{21}$.

In each sampling site, topological relations were defined within circular areas with 1 m diameter. In practice, starting from the picture of considered outcrop with a reference area, the fracture network was digitised in QGIS, and the topological characterization was defined using the "NetworkGT" toolbox developed by Nyberg et al. (2018).

Outcrop analysis was completed by determination of the Geological Strength Index (GSI). The GSI index is mainly based on the degree of interlocking of rock mass and is estimated by a direct visual examination of the rock mass using the qualitative "Hoek's

chart". One of the advantages of this index, whose values range from 0 to 100, is that the ratings can cover a wide range of rock masses and conditions moving from mechanical continuum approach to pseudo- continuum approach without losing the influence geology has on its mechanical properties.

RESULTS

The rock masses of the sampling sites are characterized by a main foliation dipping at 50° to 80° toward west and this surface was excluded from the statistical analysis because it is pervasive within all the rock masses. Dealing with the fractures crosscutting the main foliation, data obtained from scanline permitted to acquire an overall statistical analysis by discerning the preferred directions for the different types of fractures. A total of 980 fractures were measured. About 35% of total fractures consists of high angle and mainly E-W trending joints. Fractures with evidence of shear displacement are about 60% and were observed forming both isolated faults and deformation zones cm to dm wide (mesoscopic fault zones). This group includes N-S high-angle normal faults and WNW-ESE and WSW-ENE high-angle faults with a prevailing sinistral component of slip. The crack and calcite veins are the minor population of fracture types and account for 5% with predominantly WNW-ESE and EW trends (Fig. 2).

The fracture network of the sampled sites was analysed by topological analysis to quantifying nodes and branches (Fig. 3), and fracture intensity.

The fracture network of the investigated rock masses is dominated by abutting fractures, well recorded by a clear prevalence of Y-node type, and subordinate cross-cutting fractures defined by X-nodes (Fig. 3A). Therefore, the fracture networks are almost entirely formed by C–C (doubly connected) branches (Fig. 3B) marking a high level of connection among the different type of fractures. This indicate that the analysed rock masses consist of delimited blocks.

Along the section realized for fracture sampling, an increase of fractures intensity has been estimated in areas close to the
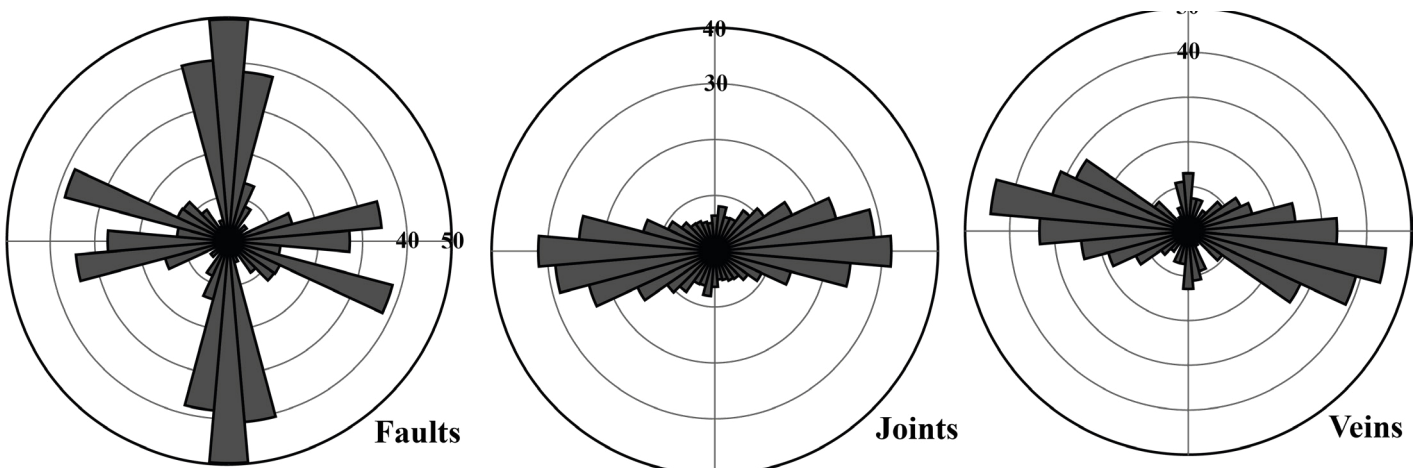

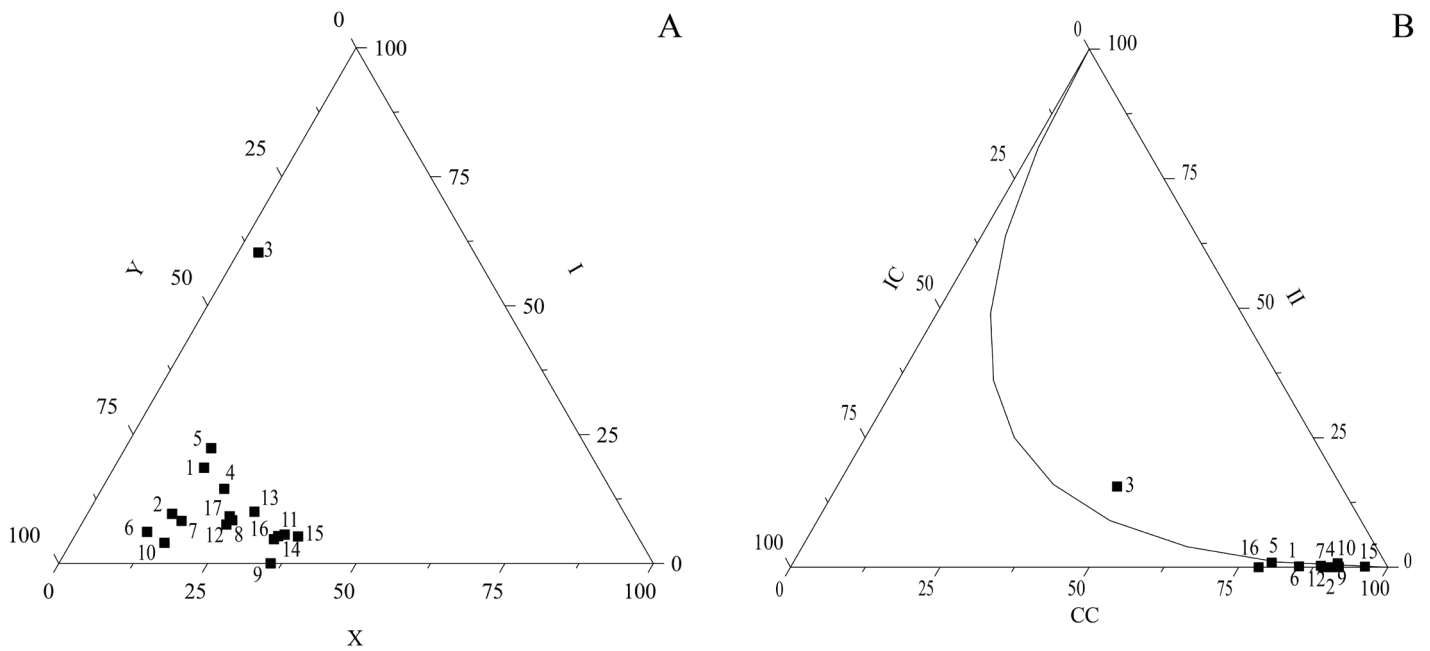Fig. 2 - Classification of type and orientation data are reported.

Fig. 3 - Ternary plots for I-X-Y nodes (a) and II-IC-CC branches (b).

two faults, indicating the potential extent of fracturing due to the faulting. These two more highly fractured zones are approximately 200 m (for the northern fault) and 400 m wide (for the southern fault) and are slightly asymmetric. Approaching these areas, the intensity values do not increase gradually but with sharp increases to values above 20 m/m2 and 70 m/m2 respectively (Fig. 4).

The interlockness degree of the blocks of investigated rock masses has been estimated considering the GSI classification chart. Sites away from the faults structure are characterised by semi-intact rock with few widely spaced, variably interacting discontinuities (GSI= 80-90). Near the faults zone, a worsening of the index affects the outcrops characterized by a decreasing interlocking of rock pieces (GSI= 40-70) to completely disaggregated rock with a mixture of angular rock pieces (GSI= 10-20) (Fig. 5).
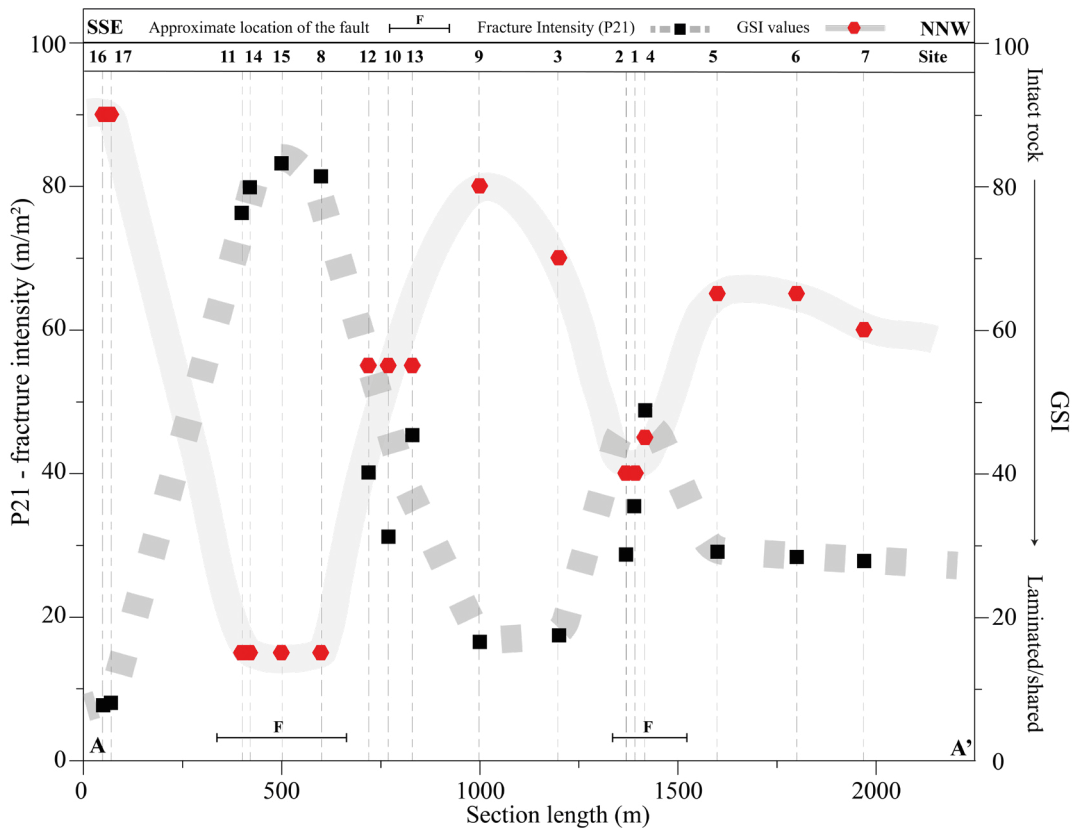

Fig. 4 - Spatial variation of P21 fracture intensity and GSI values along the A-A' section. The mapped faults are approximately located at 500 m and 1300 m from the SSE point of the realized section.
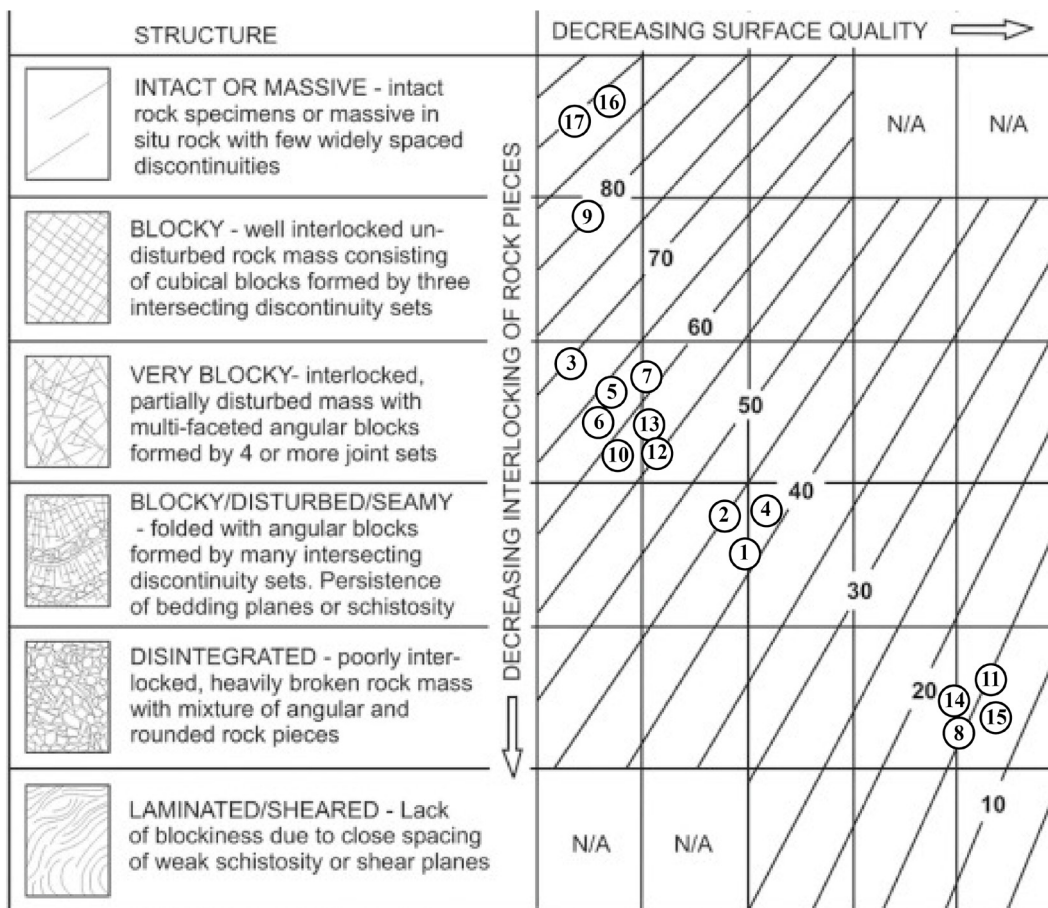
Fig. 5 - GSI classification of investigated sites (modified from Hoek at al., 1998).

CONCLUDING REMARKS

Different approaches were used to describe the fracture networks of rock masses along a section normal to the considered faults. Traditional scanline approach integrates information on fracture type and orientation with statistical treatment of fracture data set. Based on classification and counting of nodes and branches, topological analysis documents highly connected fracture networks, testified by extensive outcropping of rock masses consisting of blocks. The fracture intensity (i.e., total length of fractures per unit area) abruptly increases in areas 200 to 400 metres-wide around the considered faults. This helps to roughly delimit potential sectors with a more intense degree of fracturing and then to draw average buffer zone of the analysed fault system.

Integrating and interpolating these preliminary results with those obtained for other fault systems using the same procedure in the next steps of the ongoing project, an intensity map at regional scale will be derived. This map will give a general view of potential areas with higher occurrence of disaggregated rock masses and then the availability of loose material, which are crucial aspects to consider for the realization of landslide susceptibility maps.

The geomechanical GSI classification underlies a coherent variation in the degree of fracturing in the analysed areas close to the faults.

Declaration of competing interest

The author declares no conflict of interest.

REFERENCES

Bonetto S., Facello A., Ferrero A.M. & Umili G. (2015) - A tool for semi-automatic linear feature detection based on DTM. Computers & Geosciences, 75, 1-12.

Bonetto S., Facello A. & Umili G. (2017) - A new application of CurvaTool semi-automatic approach to qualitatively detect geological lineaments. Environmental & Engineering Geoscience, 23(3), 179-190.

Bonetto S., Mosca P., Vagnon F. & Vianello D. (2021) - New application of open source data and Rock Engineering System for debris flow susceptibility analysis. Journal of Mountain Science, 18(12), 3200-3217.

Dal Piaz G.V. (2010) - The Italian Alps: a journey across two centuries of Alpine geology. Journal of the Virtual Explorer, 36(8), 77-106.

He Y. & Beighley R.E. (2008) - GIS-based regional landslide susceptibility mapping: a case study in southern California. Earth Surf. Process. Landforms, 33, 380-393, https://doi.org/10.1002/esp.1562.

Hoek E. (1994) - Strength of rock and rock masses. News J. ISRM 2(2), 4-16.

Hoek E., Marinos P. & Benissi M. (1998) - Applicability of the geological strength index (GSI) classification for very weak and sheared rock masses. The case of the Athens Schist Formation. Bull. Eng. Geol. Environ., 57, 15-160, https://doi.org/10.1007/s100640050031.

Ilia I. & Tsangaratos P. (2016) - Applying weight of evidence method and sensitivity analysis to produce a landslide susceptibility map. Landslides, 13, 379-397, https://doi.org/10.1007/s10346-015-0576-3.

ISRM (1978) - Suggested methods for the quantitative description in rock masses. Int. J. Rock Mech. Min. Sci. Geomech. Abstr., 15, 319-368.

Jordán G., Meijninger B.M.L., Van Hinsbergen D.J.J., Meulenkamp J.E. & Van Dijk P.M. (2005) - Extraction of morphotectonic features from DEMs: Development and applications for study areas in Hungary and NW Greece. International journal of applied earth observation and geoinformation, 7(3), 163-182.

Marinos P. & Hoek E. (2000) - GSI: a geologically friendly tool for rock mass strength estimation. In ISRM international symposium. OnePetro.

Mauldon M., Dunne W.M., Rohrbaugh M.B. (2001) - Circular scanlines and circular windows: new tools for characterizing the geometry of fracture traces. J. Struct. Geol., 23, 247-258.

Nohani E., Moharrami M., Sharafi S., Khosravi K., Pradhan B., Pham B.T., Lee S. & Melesse A. (2019) - Landslide Susceptibility Mapping Using Different GIS-Based Bivariate Models. Water, 11, 1402, https://doi.org/10.3390/w11071402.

Nyberg B., Nixon C.W. & Sanderson D.J. (2018) - NetworkGT: A GIS tool for geometric and topological analysis of two-dimensional fracture networks. Geosphere, 14(4), 1618-1634.

Pahl P.J. (1981) - Estimating the mean length of discontinuity traces Int. J. Rock Mech. Min. Sci. Geomech. Abstr., 18, 221-228.

Peacock D.C.P., Sanderson D.J. & Rotevatn A. (2018) - Relationships between fractures. Journal of Structural Geology, 106, 41-53.

Pourghasemi H.R., Pradhan B. & Gokceoglu C. (2012) - Application of fuzzy logic and analytical hierarchy process (AHP) to landslide susceptibility mapping at Haraz watershed, Iran. Nat. Hazards, 63, 965-996, https://doi.org/10.1007/s11069-012-0217-2.

Priest S.D. (1993) - Discontinuity analysis for rock engineering. Springer Science & Business Media.

Priest S.D. & Hudson J.A. (1981) - Estimation of discontinuity spacing and trace length using scanline surveys. In: International Journal of Rock Mechanics and Mining Sciences & Geomechanics Abstracts, 18(3), 183-197.

Rohrbaugh Jr M.B., Dunne W.M. & Mauldon M. (2002) - Estimating fracture trace intensity, density, and mean length using circular scan lines and windows. AAPG bulletin, 86(12), 2089-2104.

Saha A.K., Gupta R.P., Sarkar I., Arora M.K. & Csaplovics E. (2005) - An approach for GIS-based statistical landslide susceptibility zonation—with a case study in the Himalayas. Landslides, 2, 61-69, https://doi.org/10.1007/s10346-004-0039-8.

Sanderson D.J. & Nixon C.W. (2015) - The use of topology in fracture network characterization. Journal of Structural Geology, 72, 55-66.

Servizio Geologico D'Italia (2020) - Carta Geologica d'Italia alla scala 1:50.0000, F. 171 Cesana Torinese. ISPRA, Roma.

Umili G., Ferrero A. & Einstein H.H. (2013) - A new method for automatic discontinuity traces sampling on rock mass 3D model. Computers & Geosciences, 51, 182-192.

Umili G., Bonetto S. & Ferrero A.M. (2018) - An integrated multiscale approach for characterization of rock masses subjected to tunnel excavation. Journal of Rock Mechanics and Geotechnical Engineering, 10(3), 513-522.

van Westen C.J., Van Duren I.C., Kruse H.M.G. & Terlien M.T.J. (1993) - GISSIZ: training package for Geographic Information Systems in slope instability zonation: Part 1. theory Part 2. exercises. ITC publication, 15.

Varnes D.J. (1978) - Slope movement types and processes. Special report, 176, 11-33.

Vianello D., Vagnon F., Bonetto S. & Mosca P. (2022) - Debris flow susceptibility mapping using the Rock Engineering System (RES) method: a case study. Landslide (in press), https://doi.org/10.1007/s10346-022-01985-6.

Wen H., Wu X., Ling S., Sun C., Liu Q. & Zhouet G. (2022) - Characteristics and susceptibility assessment of the earthquake-triggered landslides in moderate-minor earthquake prone areas at southern margin of Sichuan Basin, China. Bull. Eng. Geol. Environ., 81, 346. https://doi.org/10.1007/s10064-022-02821-w.

Wu H. & Pollard D.D. (1995) - An experimental study of the relationship between joint spacing and layer thickness. Journal of Structural Geology, 17(6), 887-905.